Removal of trimethylamine by adsorption over zeolite catalysts and deodorization of fish oil

Kyong-Hwan Chung[a], Ki-Young Lee[a,b,*]

[a] Center for Functional Nano Fine Chemicals & Department of Applied Chemical Engineering, Chonnam National University, Gwangju 500-757, Republic of Korea
[b] Department of Applied Chemical Engineering & The Research Institute for Catalysis, Chonnam National University, Gwangju 500-757, Republic of Korea

ABSTRACT

Trimethylamine (TMA) is the main agent for the odor often associated with fouling fish, some infections, and bad breath. This study focused on the adsorption of TMA over various microporous zeolites for application in the low-temperature deodorization of fishy odor from raw fish oil. The faujasite (Si/Al = 3) zeolite exhibited the high adsorption ability, which, in combination with its wide surface area and pore volume, may have induced the high adsorption ability. The H-mordenite (Si/Al = 10) zeolite exhibited a large TMA adsorption. It was considered to have generated more attractive adsorption with TMA ions, because TMA interacted briskly with cations of acid sites on the zeolites. The fishy odor of raw fish oil was considerably reduced by low-temperature adsorption on the zeolites. The surface area of the zeolites retained most of the TMA adsorption ability, and their acid strength further enhanced the adsorption ability.

© 2009 Elsevier B.V. All rights reserved.

1. Introduction

Fish oils obtained from whole fish, as well as technological fish by-products, are becoming more extensively used in feeding farm animals as they constitute a valuable ingredient of mixtures and fodder concentrates both for monogastric animals and ruminants [1–4]. Fish oils are a chief source of energy; specifically, polyunsaturated fatty acids (PUFAs) belonging to the omega-3 family are synthesized in limited quantities in the body of animals and humans and therefore are of immense physiological significance. Fish oils are rich sources of docosahexaenoic and eicosapentaenoic acids and a limited number of plant oilseeds are good sources of other PUFAs [5–7].

PUFA-containing fats and oils have peculiar, unpleasant smells. For example, fish oils have fishy smells. Thus, such oils are not used so widely in food ingredients. However, fish oils can be rendered tasteless and odorless by deodorization. It is still difficult to prevent the recurrence of fishy and other unpleasant smells. Despite the use of odor suppressors and masking agents to hide such smells, their effects are short-lived, so that they cannot offer a fundamental solution to the odor problem. It remains impossible to sufficiently suppress fishy odors.

Deodorization, the major step involving high temperatures (180–220 °C) under low pressure (1–10 mbar), is a common process used for the refining of edible fats and oils. The effect of deodorization temperature has been evaluated on the formation of long-chain PUFAs (LC-PUFAs) geometrical isomers [8,9]. Deodorization represents a critical step in the refining process as it involves high temperature that could induce degradation reactions [10,11]. Among these reactions, polymerization, geometrical isomerization and intramolecular cyclization are favored in the conditions used for deodorization of oils [10]. Cyclization, which is a minor reaction occurring in heat treated vegetable oil, has been found to be a significant, thermally induced reaction in oils containing LC-PUFAs [12–14]. This method may degrade the major component in fish oil. Therefore, research should focus on a low-temperature removal method for fishy odor to prevent fish oil from degradation.

TMA is a product of decomposition of plants and animals. With its strong fishy odor in low concentrations, TMA is the main agent for the odor often associated with fouling fish, some infections, and bad breath. It is also associated with taking large doses of choline and carnitine. Zeolites are microporous crystalline solids with well-defined structures. Generally, they contain silicon, aluminum and oxygen in their framework and cations. As catalysts, zeolites exhibit appreciable acid activity and shape selective features unlike the compositionally equivalent, amorphous catalysts [15,16]. Zeolite is an efficient adsorbent for the treatment of low concentration pollutants [17].

This study focused on the adsorption of TMA over various microporous zeolites for application in the low-temperature

* Corresponding author at: Department of Applied Chemical Engineering & The Research Institute for Catalysis, Chonnam National University, Gwangju 500-757, Republic of Korea. Tel.: +82 62 530 1843; fax: +82 62 530 1924.
E-mail address: likeu21@hanmail.net (K.-Y. Lee).

deodorization of fishy odor from raw fish oil. The TMA adsorption behaviors of various zeolite catalysts with different surface areas and acidities were investigated. The acidic properties of the zeolites with three different zeolite species and various Si/Al molar ratios were evaluated by NH$_3$ temperature programmed desorption (NH$_3$-TPD) analysis. The influences of the physicochemical properties of the zeolites on TMA removal were discussed in relation to TMA adsorption.

2. Materials and methods

2.1. Preparation of zeolite catalysts

The MFI zeolites were synthesized with four different Si/Al molar ratios through hydrothermal reaction of a synthetic mixture composed of colloidal silica (Aldrich, Ludox, 40 wt% SiO$_2$), aluminum hydroxide (Fluka, >64%), potassium hydroxide (Daejung, >85%) and deionized water. The synthetic mixture was aged for 72 h and heated at 190 °C for 48 h. The Si/Al molar ratio of the synthesized MFI zeolites ranged from 25 to 335. The other MFI zeolites were purchased from Zeolyst Co. The Na-type MFI zeolites were treated with ammonium nitrate (Duksan, >99%) of 0.5N at 60 °C to exchange their cations to ammonium ions. H-type MFI (H-MFI) zeolites were obtained by calcining at 550 °C for 6 h in air.

The mordenite zeolite (Si/Al = 10) purchased from Tosoh Co. was used as a starting material. The H-type mordenite (H-MOR) zeolites were obtained by ion exchange according to the method mentioned above. The H-type faujasite (H-FAU) zeolites were prepared from the Na-type FAU zeolite (Na-FAU; Union Carbide, Si/Al = 3) by ion exchange with a 2 M NH$_4$NO$_3$ (Aldrich, 99%) solution at 80 °C. Afterwards, the samples were filtered, washed and dried for 12 h at 100 °C. We denoted the prepared H-form zeolites according to the framework type code of the zeolites (H-MFI, H-MOR, H-FAU) and by writing their Si/Al molar ratios in parentheses after the code name.

2.2. Characterization of zeolite catalysts

The X-ray diffraction (XRD) patterns of the zeolites were recorded on an X-ray diffractometer (Rigaku D/Max Ultima III) operating under 40 kV and 40 mA with a 2°/min scan rate. Cu Kα X-ray was filtered by nickel. The morphology and sizes of the zeolites were examined by a scanning electron microscope (SEM, Hitachi S-4900). The Si/Al molar ratios of the MFI zeolites were determined using an inductively coupled plasma-atomic emission spectrometer (ICP-AES; PerkinElmer, OPTIMA 4300 DV). The values of the MOR zeolites were measured by X-ray fluorescence (PANalytical, PW1400) detection. For the purchased zeolites, the values defined by the manufacturers were adopted.

Nitrogen adsorption isotherms were obtained at liquid nitrogen temperature by an automatic volumetric adsorption system (Mirea SI, nanoPOROSITY-XQ). The zeolite samples were evacuated at 150 °C for 2 h prior to nitrogen adsorption. Thermogravimetric analysis (TGA) of the zeolites collected from the adsorption experiment after adsorption equilibrium had been reached was conducted using thermogravimetry (Metler, TGA/SDTA 851^e). TGA was performed in air condition with a ramping rate of 10 °C/min.

NH$_3$-TPD profiles of the zeolites were obtained using a chemisorption analyzer (Bel Japan, BELCAT). The zeolite samples were activated in a helium flow at 550 °C for 1 h, and then cooled to 150 °C. Ammonia pulses were supplied to the zeolite samples until saturation. The samples were purged with a helium flow at 150 °C for 1 h to remove physically adsorbed ammonia. The temperature of the zeolite sample was increased to 600 °C with a ramping rate of 10 °C/min. The number of acid sites on the zeolite surface was defined from the peak deconvolution to the measured spectrum.

2.3. TMA adsorption on the zeolites

TMA was adsorbed over the zeolites in a batch-type reactor equipped a mechanical stirrer and a water-cooled condenser. The 50 ml TMA (TCI, 28%) solution (0.1 mol/l) was charged, and then stirred in a 500 ml round bottom flask at 50 °C. Raw fish oil (50 ml) was also employed as an adsorbate in the adsorption experiment to evaluate the odor removal by adsorption. The fish oil was kindly donated by Chemport Co. (Korea). The zeolites (1.0 g) were added into the solution as an adsorbent. The stirring speed to the solution was controlled at 350 rpm. TMA concentration was analyzed by a gas chromatograph (Shimadzu, 9A) equipped with a capillary column (HP-1, i.d.: 0.32 mm, length: 50 m, film thickness: 0.17 μm) and an FID detector. The fractional TMA concentration was determined from the ratio of the TMA concentration at processing time to the initial TMA concentration.

2.4. Measurement of fishy odor

The odors of raw fish oil (20 ml) and fish oil (20 ml) deodorized by adsorption on the zeolites were measured by an odor meter (Shinyei, OMX-SR) in a hexagon box (V = 8l) controlled at 25 °C. Deodorization rate was determined from the equation as following:

$$\text{Deodorization rate (\%)} = \frac{I_{\text{raw}} - I_{\text{de}}}{I_{\text{raw}}} \times 100 \tag{1}$$

where I_{raw} means odor intensity to the raw fish oil, and I_{de} means odor intensity to the fish oil deodorized by adsorption.

3. Results and discussion

3.1. Physical properties of the zeolites

The XRD patterns of the zeolites were identical with those published in a previous literature [18], indicating that the zeolites used in this study were highly crystalline. The particle sizes of the zeolites, as defined by the SEM photos, were about 1.5 μm for the FAU and MFI zeolites, and slightly larger at 1.5–2.0 μm for the MOR zeolite. The particle size of all the zeolites was distributed in the range of 0.2–2.0 μm. Comparatively small particles were selected to obtain sufficient external surface.

The nitrogen adsorption isotherms are shown in Fig. 1. The isotherms of nitrogen on the H-MFI(25) and H-MOR(10) zeolites showed typical Langmuir characteristics, which is a usual adsorption isotherm for zeolites since their micropores are filled
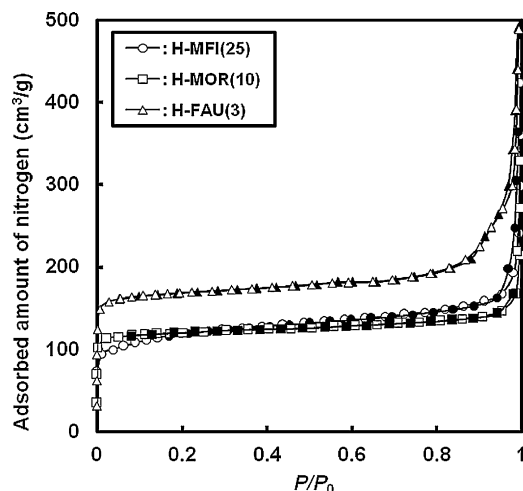

Fig. 1. N$_2$ isotherms of the zeolites.

Table 1
Structural properties and adsorption amounts of TMA on the zeolites.

Zeolite	Pore size (Å)	BET surface area (m²/g)	Micropore volume[a] (cm³/g)	Amount of TMA adsorbed on the zeolite[b] (mg/g of zeolite)
H-FAU(3)		574	0.23	87.7
Na-FAU(3)	7.4 × 7.4[1 1 1]	571	0.22	33.4
H-MOR(10)	6.5 × 7.0[0 0 1]	419	0.17	63.9
Na-MFI(25)		415	0.12	21.3
H-MFI(25)		413	0.12	26.5
H-MFI(46)	5.1 × 5.5[1 0 0], 5.3 × 5.6[0 1 0]	405	0.13	20.1
H-MFI(75)		407	0.13	14.7
H-MFI(335)		418	0.14	3.0

[a] The values were determined from the nitrogen adsorption isotherm using Saito–Foley method [24].

[b] These values were determined from the TGA results for the zeolites collected from the adsorption experiments after adsorption equilibrium of TMA had been reached.

with adsorbed nitrogen even at very low pressures. The large adsorption on the H-FAU(3) zeolites was attributed to their large void fraction. The Brunauer–Emmett–Teller (BET) surface area and micropore volume determined from the isotherms are summarized in Table 1. The FAU(3) zeolite had the largest surface area. The MFI zeolite had a narrow pore entrance compared with that of the other zeolites, and its pore shape resembled a bent pore channel with a zigzag type. The MOR zeolite had a wide pore entrance and a straight pore channel. Nevertheless, the surface areas of the two zeolites were similar apart from their pore structure.

3.2. Acidic properties of the zeolites

The acidic properties of the zeolites varied according to the zeolite species, even though the Si/Al molar ratios of the zeolites had been controlled to be similar. Fig. 2 shows the NH₃-TPD profiles of the three zeolite species and of the H-MFI zeolites with four Si/Al molar ratios. The TPD technique is widely used to examine the general acidic feature of a catalyst [19–21]. The number of acid sites of the catalysts can be determined from the desorption peak area of ammonia. Acid strength can be evaluated by the maximum peak temperature (T_{max}) of the desorption peak in relation to the activation energy for the desorption of ammonia.

The desorption peaks observed at 350–550 °C were attributed to strong acid sites, whereas those at 150–250 °C revealed weak acid sites or physically adsorbed ammonia. The H-MOR zeolites exhibited acid sites that were larger and stronger than those of the other zeolites, as shown in Fig. 2(A). The FAU(3) zeolites only had many weak acid sites. It revealed that the acid strength of the Na-type zeolites was weaker than that of H-type zeolites. The number of strong acid sites varies according to the spatial conformations of the Si–O–Al bonds determined by zeolite skeletal, while the number of acid sites is related to the Si/Al molar ratio [20].

In order to evaluate the adsorption properties on the same zeolite species with various acidities, the H-MFI zeolites with four different Si/Al ratios were employed in the reaction. The NH₃-TPD profiles of the four H-MFI zeolites are shown in Fig. 2(B). The strong acid sites of the H-MFI zeolites were significantly decreased with decreasing Al content in the zeolite framework. In addition, the T_{max} of the strong acid site was slightly shifted toward a lower temperature. Katada et al. [22,23] suggested that the acid strength can be defined as ΔH in their proposed theoretical thermodynamic equation. They proposed that T_{max} is affected by the $A_0 W/F$, where A_0 means the number of acid sites, W means amount of catalyst, and F is a flow rate of ammonia. If the W/F was fixed, the T_{max} is affected by the number of acid sites (A_0). Therefore, it seems that the small variation in T_{max} of NH₃-TPD between H-MFI zeolites with a large difference of the number of acid sites was due to the difference of the number of acid sites.

3.3. TMA adsorption on the zeolites

Fig. 3 shows the TMA adsorption behaviors of the zeolites. The fractional concentration indicates the ratio of TMA concentration at processing time to the initial TMA concentration. The adsorption behaviors of TMA on the three zeolite species (MFI, MOR, FAU) are shown in Fig. 3(A). The TMA adsorption on the zeolites reached an equilibrium after 10 h. More than 80% of the TMA was adsorbed on all three H-FAU(3), Na-FAU(3), and H-MOR(10) zeolites, with the former zeolite exhibiting the largest TMA adsorp-
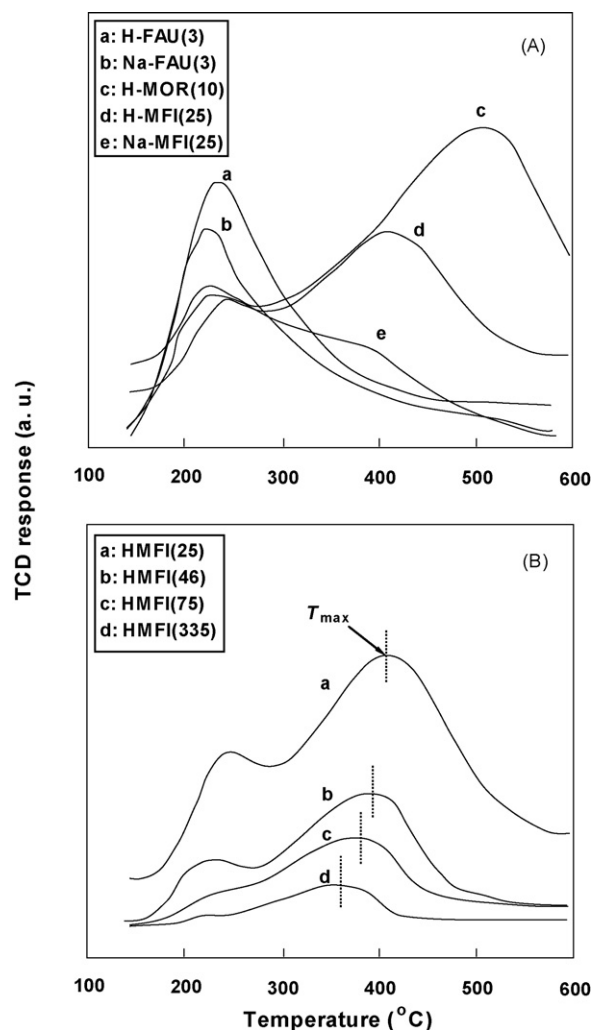

Fig. 2. NH₃-TPD profiles (A) of the three zeolite species, and of the H-MFI zeolites with four different Si/Al molar ratios (B).
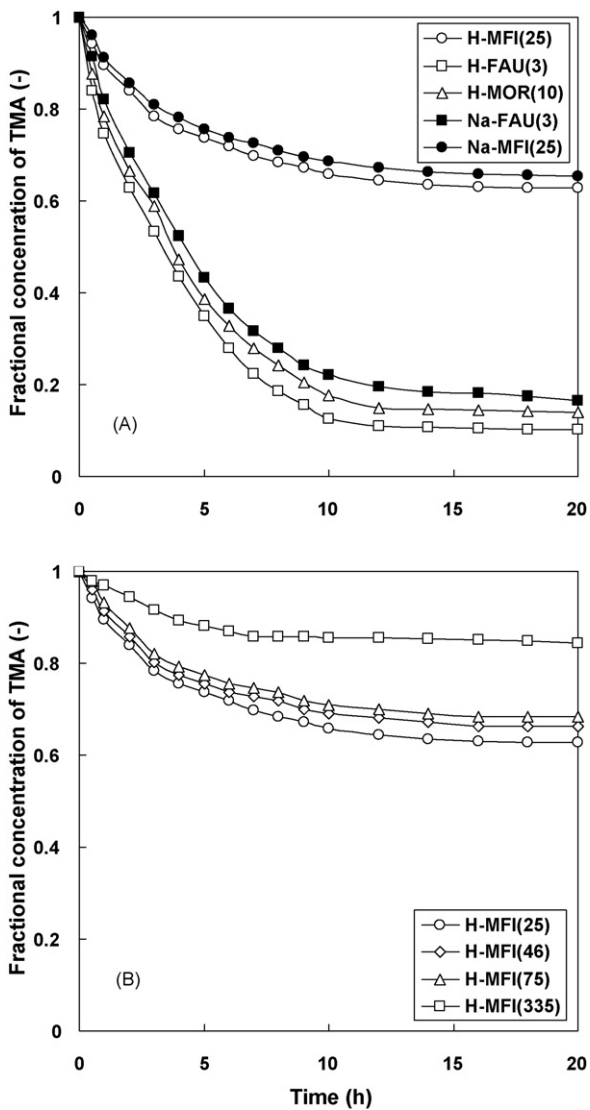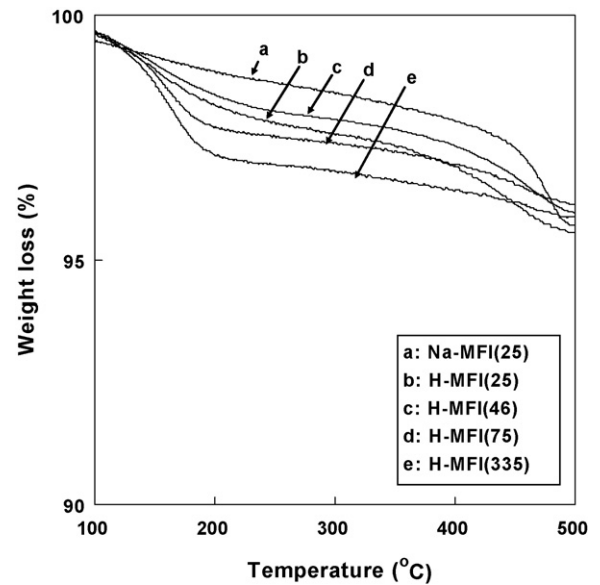
Fig. 4. TGA results of the zeolites collected from the adsorption experiments.

tion ability. The adsorption ability improved with decreasing Si/Al molar ratio.

Fig. 4 shows the TGA results of the zeolites collected from the TMA adsorption experiment after adsorption equilibrium had been reached. The weight loss of the zeolites at 100–150 °C was derived from the vaporization of water sorbed on the zeolites. The second weight loss appeared from 300 to 500 °C was derived from the desorption of TMA adsorbed on the zeolites. The amount of this second weight loss indicates the amounts of TMA adsorption on the zeolites, which are listed in Table 1. The adsorption was largest on the H-FAU(3) zeolite. In the H-MFI zeolites with four different Si/Al molar ratios, which have similar surface areas, the TMA adsorption amount decreased with decreasing acid strength of the H-MFI zeolites.

The temperature programmed desorption of TMA (TMA-TPD) on the H-MFI zeolites with four different Si/Al molar ratios is shown in Fig. 5. The desorption curves of TMA-TPD were determined from the TGA results of the zeolites that had adsorbed TMA. The desorption peak shown at 350–500 °C was attributed to the desorption of

Fig. 3. Fractional concentration of adsorbed TMA (A) on the three zeolites, and (B) on the H-MFI zeolites with four different Si/Al molar ratios.

tion of all. The FAU zeolite has a weaker acid strength, compared to the other zeolites, but a wider pore size and a larger surface area. Moreover, the FAU zeolite has a void supercage in its pore structure, which, in combination with its wide surface area, may have induced the high adsorption ability. Therefore, we attributed the high TMA adsorption of the H-FAU zeolite to its large surface area.

Despite having a small surface area of size similar to that of the H-MFI zeolite, the H-MOR(10) zeolite exhibited a large TMA adsorption compared to the H-MFI zeolites. The H-MOR(10) zeolite has stronger acid sites than those of the other zeolites, as shown in the NH_3-TPD results (see Fig. 2(A)), and this increased strength was considered to have generated more attractive adsorption with TMA ions, because TMA interacts briskly with cations of acid sites on the zeolites. Therefore, the H-MOR(10) zeolite adsorbed as much TMA as the FAU(3) zeolite did, despite its smaller surface area. This indicated that both the acid strength and the surface area of the zeolites affected the TMA adsorption. The TMA adsorption behaviors on the H-MFI zeolites with the four Si/Al molar ratios are shown in Fig. 3(B). The zeolite acidity decreased with increasing Si/Al molar ratio, because the Al atoms acted as the acid sites in the zeolite framework. The H-MFI(25) zeolite exhibited the highest adsorp-
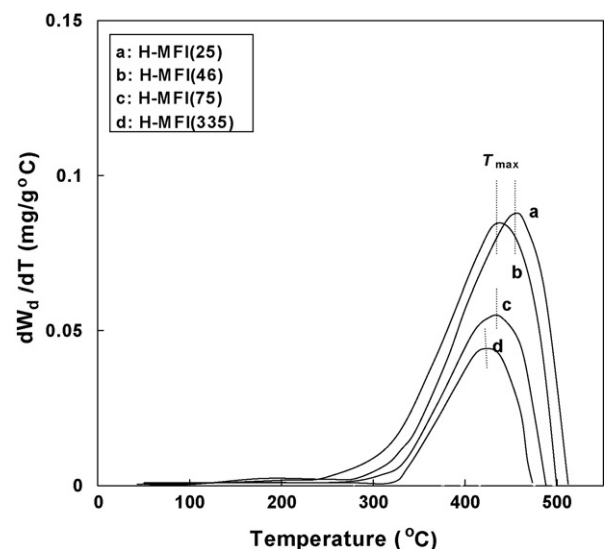

Fig. 5. TMA-TPD of the H-MFI zeolites with four different Si/Al molar ratios.

TMA on the acid sites of the zeolites. The desorption peaks increased with increasing Al content in the zeolite framework. The H-MFI(25) and H-MFI(46) zeolites exhibited a similar magnitude of desorption peaks, but the T_{max} of the former was higher than that of the latter, which was due to the difference of their acid site contents, as defined in the NH$_3$-TPD results. Therefore, the TMA adsorption amount on the H-MFI(25) zeolite was larger than that of the H-MFI(46) zeolite, as shown in Fig. 3(B). With increasing Si/Al molar ratio, the desorption peaks were reduced and the T_{max} of the zeolites was slightly shifted toward a lower temperature. These results represent further evidence suggesting that the number of acid sites can increase the TMA adsorption on the same zeolite species.
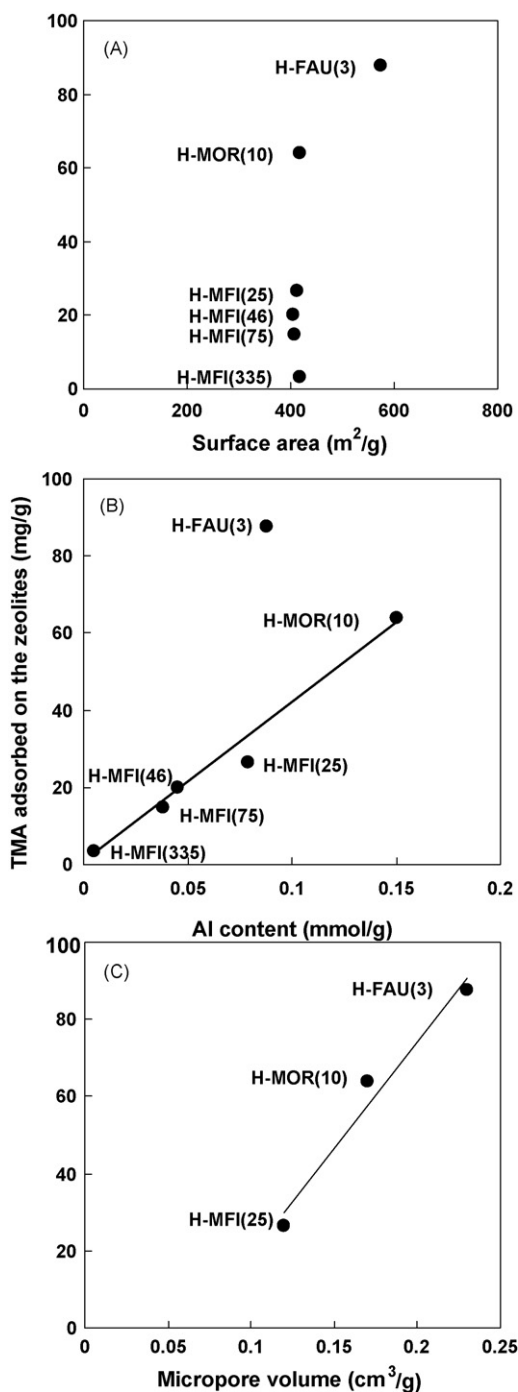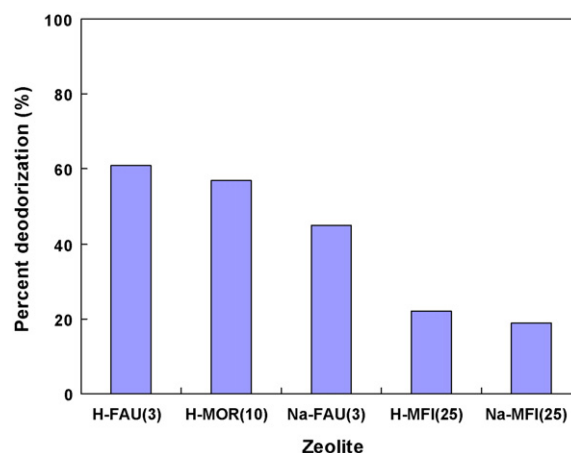

Fig. 7. Deodorization rate of raw fish oil by adsorption on the zeolites at 50 °C.

Fig. 6 shows the TMA adsorbed on the zeolites related to the physical properties of the zeolites. The adsorption of TMA on the zeolites did not show a relationship with the surface area of the zeolites as shown in Fig. 6(A). The adsorption amount of TMA increased with increasing the number of acid sites in the H-MOR and H-MFI zeolites which have similar surface areas and micropore volumes (Fig. 6(B)), except for the H-FAU(3) zeolite. On the contrary, the adsorption amount of TMA was increased in proportional with their micropore volume in the adsorption of the different zeolite species such as H-FAU, H-MOR, and H-MFI zeolites (Fig. 6(C)). It seems that a lager difference of micropore volume led the difference of adsorption abilities for TMA on the zeolites, and the number of acid sites affected to the adsorption abilities for the TMA on the zeolites which have similar physical properties such as micropore volume and surface area.

3.4. Deodorization of fish oil by adsorption

The results of the deodorization of fish oils by adsorption on the zeolites are shown in Fig. 7. The deodorization efficiency was high on the H-FAU(3) zeolites, in line with the TMA adsorption results shown in Fig. 3(A). Approximately 60% of the odor of the raw fish oil was removed by adsorption on the H-FAU(3) zeolite at 50 °C, indicating the potential of the zeolite adsorption ability to considerably remove the fishy odor in fish oil. To summarize the study results, the fishy odor of raw fish oil was effectively reduced by low-temperature adsorption on zeolites without the fish oil suffering any degradation reaction.

4. Conclusions

The zeolite catalysis demonstrated an ability to remove 65% of the TMA by adsorption in solution. The TMA adsorption ability of the zeolites decreased in the following order: H-FAU > H-MOR > H-MFI zeolite. This result was explained by fact that the micropore volume of the zeolites retains most of the TMA adsorption ability, and their number of acid sites further enhanced the adsorption ability. The TMA adsorption was larger on the H-type zeolites than on the Na-type zeolites. The fishy odor was considerably reduced by low-temperature adsorption on zeolites.

Acknowledgements

Fig. 6. Relationship between TMA adsorption and the structural properties: (A) surface area, (B) Al content, and (C) micropore volume.

References

[1] R. Gonzales-Esquerra, S. Lesson, Effect of menhaden oil and flaxseed in broiler diets on sensory quality and lipid composition of poultry meat, Br. Poult. Sci. 41 (2000) 481–488.

[2] R. Baer, J. Ryali, D. Schingoethe, K. Kasperson, D. Donovan, A. Hippen, S. Franklin, Composition and properties of milk and butter from cows fed fish oil, J. Dairy Sci. 84 (2001) 345–353.

[3] E.A. Bryhni, N.P. Kjos, R. Ofstad, M. Hunt, Polyunsaturated fat and fish oil in diets for growing–finishing pigs: effects on fatty acid composition and meat, fat, and sausage quality, Meat Sci. 62 (2002) 1–8.

[4] A. Korniewicz, Z. Dobrzanski, R. Kołacz, D. Korniewicz, Z. Usydus, Usefulness of modified fish meal (MFM) in feeding of fattening pigs, Ann. Anim. Sci. 2 (2002) 139–148.

[5] R.G. Ackman, W. Ratnayake, Non-enzymatic oxidation of seafood lipids, in: Advances in Seafood Biochemistry: Composition and Quality, Technomic Publishing Co. Inc., Lancaster, 1992, pp. 245–267.

[6] D. Allen, Fish oil compositions, Fish Oil Technol. Nutr. Market (1995) 95–108.

[7] W.J. Chen, S.L. Yeh, Effects of fish oil in parental nutrition, Nutrition 19 (2003) 275–279.

[8] V. Fournier, P. Juanéda, F. Destaillats, F. Dionisi, P. Lambelet, J.-L. Sébédio, O. Berdeaux, Analysis of eicosapentaenoic and docosahexaenoic acid geometrical isomers formed during fish oil deodorization, J. Chromatogr. A 1129 (2006) 21–28.

[9] G. Henon, Z. Kemeny, K. Recseg, F. Swobada, K. Kovari, Degradation of α-linolenic acid during heating, J. Am. Oil Chem. Soc. 74 (1997) 1615–1617.

[10] R.L. Wolff, Alpha-linolenic acid geometrical isomers in deodorized oils: occurrence, characteristics, and biochemical effects, Recent Res. Dev. Oil Chem. 1 (1997) 127–148.

[11] J. Cmolik, J. Pokorny, Physical refining of edible oils, Eur. J. Lipid Sci. Technol. 102 (2000) 472–486.

[12] V. Fournier, F. Destaillats, P. Juaneda, F. Dionisi, P. Lambelet, J.L. Sébédio, O. Berdeaux, Thermal degradation of long-chain polyunsaturated fatty acids during deodorization of fish oil, Eur. J. Lipid Sci. Technol. 108 (2006) 33–42.

[13] O. Berdeaux, V. Fournier, P. Lambelet, F. Dionisi, J.L. Sébédio, F. Destaillats, Isolation and structural analysis of the cyclic fatty acid monomers formed from eicosapentaenoic and docosahexaenoic acids during fish oil deodorization, J. Chromatogr. A 1138 (2007) 216–224.

[14] W.M.N. Ratnayake, Overview of methods for the determination of *trans* fatty acids by gas chromatography, silver-ion thin-layer chromatography, silver-ion liquid chromatography, and gas chromatography/mass spectrometry, J. AOAC Int. 87 (2004) 523–539.

[15] S.J. Kim, M.J. Park, K.-D. Jung, O.-S. Joo, Catalytic performance of metal-substituted ZSM-5 zeolites for vapor phase Beckmann rearrangement of cyclohexanone oxime, J. Ind. Eng. Chem. 10 (2004) 995–1002.

[16] H.J. Park, J.-I. Dong, J.-K. Jeon, K.-S. Yoo, J.-H. Yim, J.-M. Sohn, Y.-K. Park, Conversion of the pyrolytic vapor of radiata pine over zeolites, J. Ind. Eng. Chem. 13 (2007) 182–189.

[17] V.F. Medina, T. Webster, J.S. Devinny, Treatment of gasoline residuals by granular activated carbon based biological filtration, J. Environ. Sci. Health Part A 30 (1995) 407–412.

[18] M.M.J. Treacy, J.B. Higgins, Collection of Simulated XRD Powder Patterns for Zeolites, 5th ed., Elsevier, New York, 2007.

[19] Y. Miyamoto, N. Katada, M. Niwa, Acidity of β zeolite with different Si/Al$_2$ ratio as measured by temperature programmed desorption of ammonia, Micropor. Mesopor. Mater. 40 (2000) 271–281.

[20] M. Niwa, S. Nishikwa, N. Kadata, IRAMS-TPD of ammonia for characterization of acid site in β-zeolite, Micropor. Mesopor. Mater. 82 (2005) 105–112.

[21] K.-H. Chung, Dealumination of mordenites with acetic acid and their catalytic activity in the alkylation of cumene, Micropor. Mesopor. Mater. 111 (2008) 544–550.

[22] N. Katada, H. Igi, J.-H. Kim, M. Niwa, Determination of the acidic properties of zeolite by theoretical analysis of temperature-programmed desorption of ammonia based on adsorption equilibrium, J. Phys. Chem. B 101 (1997) 5969–5977.

[23] N. Katada, T. Tsubaki, M. Niwa, Measurements of number and strength distribution of Brønsted and Lewis acid sites on sulfated zirconia by ammonia IRMS-TPD method, Appl. Catal. A: Gen. 340 (2008) 76–86.

[24] A. Saito, H.C. Foley, Curvature and parametric sensitivity in models for adsorption in micropores, AIChE J. 37 (1991) 429–436.